A theoretical study on spin-dependent transport of 'ferromagnet/carbon nanotube encapsulating magnetic atoms/ferromagnet' junctions with four-valued conductances

2004 J. Phys.: Condens. Matter 16 5605

(http://iopscience.iop.org/0953-8984/16/30/020)

INSTITUTE OF PHYSICS PUBLISHING JOURNAL OF PHYSICS: CONDENSED MATTER

J. Phys.: Condens. Matter **16** (2004) 5605–5614 PII: S0953-8984(04)79148-1

A theoretical study on spin-dependent transport of 'ferromagnet/carbon nanotube encapsulating magnetic atoms/ferromagnet' junctions with four-valued conductances

Satoshi Kokado[1,2] **and Kikuo Harigaya**[2,3]

[1] Faculty of Engineering, Shizuoka University, Hamamatsu 432-8561, Japan
[2] Nanotechnology Research Institute, AIST, Tsukuba 305-8568, Japan
[3] Synthetic Nano-Function Materials Project, AIST, Tsukuba 305-8568, Japan

E-mail: tskokad@ipc.shizuoka.ac.jp and k.harigaya@aist.go.jp

Received 12 April 2004
Published 16 July 2004
Online at stacks.iop.org/JPhysCM/16/5605
doi:10.1088/0953-8984/16/30/020

Abstract

As a novel function of ferromagnet (FM)/spacer/FM junctions, we theoretically investigate a multiple-valued (or multi-level) cell property which is in principle realized by sensing conductances of four states recorded with magnetization configurations of two FMs: (up, up), (up, down), (down, up), and (down, down). In order to sense all the states, four-valued conductances corresponding to the respective states are necessary. We previously proposed that four-valued conductances are obtained in FM1/spin-polarized spacer (SPS)/FM2 junctions, where FM1 and FM2 have different spin polarizations, and the spacer depends on spin (Kokado and Harigaya 2003 *J. Phys.: Condens. Matter* **15** 8797). In this paper, an ideal SPS is considered as a single-wall armchair carbon nanotube encapsulating magnetic atoms, where the nanotube shows on-resonance or off-resonance at the Fermi level according to its length. The magnitude of the obtained four-valued conductances has an opposite order between the on-resonant nanotube and the off-resonant one, and this property can be understood by considering electronic states of the nanotube. Also, the magnetoresistance ratio between (up, up) and (down, down) can be larger than the conventional one between parallel and anti-parallel configurations.

1. Introduction

Spin-polarized junctions (SPJs) such as ferromagnet (FM)/spacer/FM junctions [1–4] have been recently applied to elements in magnetic random access memories (MRAM) because of their magnetoresistance (MR) effect, which appears when an applied magnetic field changes

the angle between magnetizations of two FMs. In practical use, a spin-valve type, which corresponds to a memory cell of two values (one bit) represented by '0' and '1' [5], is usually adopted. For the writing process, the magnetization of only one side of the FM is changed under the applied field so that magnetization configurations between two FMs are parallel (P) or anti-parallel (AP). For the reading process, we use the difference in resistance between the P and AP configurations, the so-called MR effect.

For the SPJ, much effort has been made to develop elements in high density memories, which also have high sensitivity for the reading process. Important factors are considered to be (a) large MR ratio, whose expression as a percentage is defined by $100 \times (\Gamma_{\rm P} - \Gamma_{\rm AP})/\Gamma_{\rm AP}$ with $\Gamma_{\rm P\ (AP)}$ being the conductance of the P (AP) case, and (b) ultra-small junctions. A realistic SPJ for (a) can be, for example, Co–Fe/Al–O/Co–Fe junctions with an MR ratio of 60% at room temperature [2], epitaxially grown $Ga_{1-x}Mn_xAs/AlAs/Ga_{1-x}Mn_xAs$ junctions with an MR ratio more than 70% at 8 K [3], and Co/Fe-doped $Al_2O_3/Ni_{80}Fe_{20}$ junctions, whose MR ratio was enhanced as compared to the case of an undoped Al_2O_3 [4]. On the other hand, candidates for the SPJ for (b) may be FM/nanowire/FM junctions and FM/carbon nanotube/FM junctions [6–11], where it should be noted that the nanotube length is about 200 nm [7, 8] or 250 nm [6] in actual experiments and their size is very large at the present moment. In the future, however, we expect many problems with how to miniaturize the junctions, because challenges for the limits of the junctions size will be more and more severe in spite of the progress of experimental techniques.

Studies from other viewpoints far from the miniaturization are necessary simultaneously. In fact, for other memories [12] such as the Flash memory [13], the multiple-valued (or multi-level) cell property [13], which allows the plural bits to be stored in each memory cell and accordingly reduces the memory cell size by 1/(the number of bits), has been extensively studied. On the other hand, there are few studies for the SPJ. If such a property is included in the SPJ, it will function as a memory cell which is more efficient than the conventional one.

We here describe the multiple-valued cell property in the general SPJ, based on our previous study [14]. In a possible scheme, recorded states are supposed to be four magnetization configurations of two FMs consisting of (up, up), (up, down), (down, up), and (down, down), which are obtained by applying the magnetic fields to the respective FMs. The junctions correspond just to two-bit memory cells. Then, in order to sense all the states, four-valued conductances corresponding to the respective states are obviously necessary. By paying attention to the magnitude of total magnetization in the whole system, a model to obtain such conductances is considered to be FM1/spin-polarized spacer (SPS)/FM2 junctions, where FM1 and FM2 have different spin polarizations[4], according to the following procedure. First, a difference of conductances between (up, up) and (down, down) will appear, if the spacer is the SPS, where magnetization in the spacer is pinned. Second, a difference between (up, down) and (down, up) will be obtained by introducing FM1 and FM2, in addition to the above mentioned SPS.

In this paper, as an ideal SPS to observe four-valued conductances, we adopt a single-wall armchair carbon nanotube encapsulating magnetic atoms [16, 17], and investigate the spin-dependent transport of 'FM1/single-wall armchair carbon nanotube encapsulating magnetic atoms/FM2' junctions using the Green function technique. When all spins of magnetic atoms are pinned parallel to the magnetization axes of FM1 and FM2, four-valued conductances are explicitly obtained at a certain value of an exchange interaction between conduction electron spin and magnetic atom spin. The magnitude of the obtained four-valued conductances has

[4] The spin polarization is defined by $P_{1\ (2)} = (D_{1\ (2),\uparrow} - D_{1\ (2),\downarrow})/(D_{1\ (2),\uparrow} + D_{1\ (2),\downarrow})$, where $D_{1\ (2),\uparrow}$ is the density of states (DOS) at the Fermi level of FM1 (2) for spin up and $D_{1\ (2),\downarrow}$ is that of FM1 (2) for spin down. Also, for the spin polarization at the interfacial layer, the DOS at the interfacial layer is used as $D_{1\ (2),\uparrow}$. For example, see [15].

an opposite order between a nanotube with on-resonant behaviour and one with off-resonant behaviour. Also, the MR ratio between $\Uparrow$, $\Uparrow$ and $\Downarrow$, $\Downarrow$ can be larger than the conventional one between P and AP configurations.

2. Ideal spin-polarized spacers to obtain four-valued conductances

We first consider ideal SPSs to certainly observe four-valued conductances. In the previous study [14], we found that four-valued conductances tend to be obtained in the case of a largely spin-polarized spacer with

$$\frac{T_{\uparrow,\uparrow} - T_{\downarrow,\downarrow}}{T_{\uparrow,\uparrow}} \sim 1, \tag{1}$$

where $T_{\uparrow,\uparrow}$ and $T_{\downarrow,\downarrow}$ are spin-up and spin-down transmission coefficients, respectively, in an expression of the conductance [18, 19],

$$\Gamma = \frac{4\pi^2 e^2}{h} \sum_{\sigma=\uparrow,\downarrow} \sum_{\sigma'=\uparrow,\downarrow} T_{\sigma,\sigma'} D_{1,\sigma}(E_{\mathrm{F}}) D_{2,\sigma'}(E_{\mathrm{F}}), \tag{2}$$

with σ ($=\uparrow$ or $\downarrow$) being the spin of the conduction electron, $D_{1\ (2),\sigma}(E)$ being the local density of states (DOS) at an interfacial layer in FM1 (2) at the Fermi level E_{F}, and $T_{\sigma,\sigma'}$ being a spin-dependent transmission coefficient including the spin-flip process of $\sigma \neq \sigma'$. Based on this fact, we give four objectives for the spacer having magnetic atoms, which are

(i) to strongly pin the magnetization of magnetic atoms in the spacer parallel to magnetization axes of FMs,
(ii) to diminish magnetic couplings between magnetic atoms and FMs,
(iii) to make effective couplings between the conduction electron spin and spins of magnetic atoms, which act as much as possible, and
(iv) to have a long spin-flip scattering length to conserve the spin of conduction electron through the spacer.

As for (i), we propose that a coercive field of magnetic particles consisting of magnetic atoms is much higher than those of FMs. For (ii), we suppose that distances between magnetic atoms and FMs should be controlled so that magnetic dipole–dipole interactions between them become very small and have little influence on the spin-dependent conduction. In (iii), we should make a situation so that electrons in all conduction routes can interact with spins of magnetic atoms. For (iv), it is desired that the spin–orbit interaction of a material of the spacer is very small.

As a realistic SPS, which could satisfy such objectives, we bear in mind a carbon nanotube encapsulating magnetic atoms [16, 17] for the following reasons: first, the size of a particle consisting of magnetic atoms may be close to that of a single-domain particle by tuning conditions of fabrication, where the single-domain particle has a high coercive field. The coercive field was recently observed as about 0.5 kOe at 300 K even for Fe particles encapsulated with non-single-domain size of about 70 nm [16]. Furthermore, for only the magnetic particle, it was experimentally shown that the Fe_2O_3 nanoparticle with the diameter of 6.3 nm has the coercive field of 1 kOe at 300 K [20]. If such a particle can be encapsulated in the nanotube, the nanotube will act as an ideal SPS. Second, magnetic atoms can be encapsulated in the inner region of the nanotube [16], where distances between the atoms and nanotube edges could be tuned by controlling nanotube growth processes. Third, since the encapsulated magnetic atoms are completely surrounded by carbon atoms, electrons in all conduction routes can interact with spins of magnetic atoms. Here, the magnitudes of couplings may also be tunable by controlling nanotube growth processes, because they strongly depend on distances

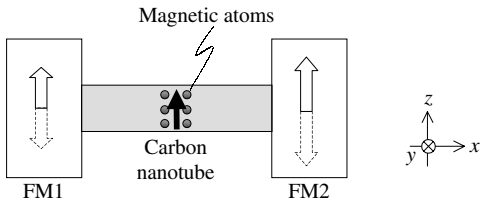

Figure 1. A schematic illustration of spin-polarized junctions with the carbon nanotube, where magnetic atoms are encapsulated in the centre of the nanotube. Electric currents flow in the x-direction.

between carbon atoms and magnetic atoms. Fourth, the nanotube itself has very long spin-flip scattering lengths which extend to 130 nm at least [6].

3. 'FM1/carbon nanotube encapsulating magnetic atoms/FM2' junctions

3.1. Model and method

We focus on 'FM1/single-walled armchair carbon nanotube encapsulating magnetic atoms/FM2' junctions, where magnetic atoms are located in the centre of the nanotube. Figure 1 shows a simplified model, in which the FM has a simple cubic structure, the x-direction of FMs is set to be semi-infinite, and their yz-directions have the periodic boundary condition by being regarded as an infinite system. The armchair nanotube has a finite length, and then it is regarded just as an armchair ribbon [21] with short periodicity. Each edge carbon atom of the nanotube is assumed to interact with its nearest atom of the cubic lattice of the FM. On the other hand, the encapsulated magnetic atoms have localized spins. We here assume that their spins are divided into several spin clusters which interact with their nearest carbon atoms respectively, and all the spin clusters have identical total spin. The total spin is approximately represented by a classical spin **S** on the assumption that the spin cluster consists of many spins, and further every **S** is set to have the same direction. Now, each **S** is arrayed along two dimer lines of the nanotube, and it has one to one interaction with carbon atoms in their lines. According to the theory on the magnetic impurity problem [22], we take into account antiferromagnetic exchange interactions between conduction electron spins and spins **S**, where all the exchange interactions are here set to be the same. Also, interactions between spins **S** and spins of FMs are neglected by assuming that they have little influence on the spin-dependent conduction, under a balance between their coercive fields and magnetic fields due to respective spins. The balance is actually sensitive to distances between magnetic atoms and FMs.

Using a single-orbital tight binding model with nearest neighbour transfer integrals, the Hamiltonian is given by

$$H_{\text{total}} = H + V, \tag{3}$$

$$H = H_1^0 + H_2^0 + H_{\text{NT}}, \tag{4}$$

$$H_{\text{NT}} = H_{\text{NT}}^0 + H_{\text{mag}}, \tag{5}$$

with

$$H_u^0 = \sum_{i\in u}\sum_{\sigma} e_{i,\sigma} c_{i,\sigma}^{\dagger} c_{i,\sigma} + \sum_{\langle i,j\rangle\in u}\sum_{\sigma} (t_{i,j} c_{i,\sigma}^{\dagger} c_{j,\sigma} + \text{h.c.}), \tag{6}$$

for u =1, 2, NT,

$$H_{\text{mag}} = \sum_{i\in\text{mag}} \left(\Delta e \sum_{\sigma} c_{i,\sigma}^{\dagger} c_{i,\sigma} - J \sum_{\sigma,\sigma'} \boldsymbol{\sigma}_{\sigma,\sigma'} \cdot \mathbf{S} c_{i,\sigma}^{\dagger} c_{i,\sigma'} \right), \tag{7}$$

$$V = \sum_{\langle i,j \rangle} \sum_{\sigma} (v_{i,j} c^{\dagger}_{i,\sigma} c_{j,\sigma} + \text{h.c.}), \tag{8}$$

where $H^0_{1\,(2)}$ is the Hamiltonian for FM1 (FM2), $H^0_{\rm NT}$ is that for the carbon nanotube, and $H_{\rm mag}$ denotes interactions between the encapsulated magnetic atoms and the respective nearest carbon atoms, where $\sum_{i\in{\rm mag}}$ means that the summation is taken for carbon atoms interacting with magnetic atoms. The term V represents couplings between FMs and the nanotube, where each edge carbon atom of the nanotube couples to its nearest atom of the cubic lattice of the FM. Here, $c_{i,\sigma}$ ($c^{\dagger}_{i,\sigma}$) is the annihilation (creation) operator of an electron with spin σ (=$\uparrow$ or $\downarrow$) at the ith site, $t_{i,j}$ and $v_{i,j}$ are transfer integrals between the ith site and the jth site, and $e_{i,\sigma}$ denotes the on-site energy for spin σ at the ith site. Furthermore, Δe is the difference of energy between the pure carbon atom and the carbon atom interacting with the magnetic atoms, J is the antiferromagnetic exchange integral with negative sign [22], and $\sigma_{\sigma,\sigma'}$ is the (σ,σ') component of the Pauli matrix for the conduction electron spin. Also, $\mathbf{S}$ [=(S_x, S_y, S_z)] represents the classical spin with $S \equiv |\mathbf{S}|$.

Within the Green function technique [18, 19], we calculate the conductance at zero temperature, which is written as

$$\Gamma = \frac{4\pi^2 e^2}{h} \text{Tr}[\hat{D}_1 \hat{T}^{\dagger} \hat{D}_2 \hat{T}], \tag{9}$$

$$\hat{T} = V + V G^{\dagger} V, \tag{10}$$

$$G = (E_{\rm F} + \text{i}0 - H_{\rm total})^{-1}, \tag{11}$$

with

$$\hat{D}_u = -\frac{1}{\pi} \text{Im}\, G^0_u, \tag{12}$$

$$G^0_u = (E_{\rm F} + \text{i}0 - H^0_u)^{-1}, \tag{13}$$

for $u = 1, 2$. Here, $\hat{D}_{1\,(2)}$ is the density-of-states (DOS) operator at $E_{\rm F}$ of FM1 (2), and $\hat{T}$ is the T-matrix. We below denote Γ for the respective magnetization configurations as $\Gamma_{m1,m2}$, where $m1$ ($m2$) is the magnetization state of FM1 (FM2), which is $\Uparrow$ or $\Downarrow$.

Using these conductances, we obtain the MR ratio as a percentage, which is defined by

$$R_{m1,m2} = 100 \times \frac{\Gamma_{\Downarrow,\Downarrow} - \Gamma_{m1,m2}}{\Gamma_{\Downarrow,\Downarrow}}, \tag{14}$$

where $m1$ ($m2$) is the magnetization state of FM1 (FM2) with $\Uparrow$ or $\Downarrow$.

In this calculation, we choose parameters as follows: we set[5] $t_{i,j} = t$ (<0) and $v_{i,j} = 0.1t$, assuming that v is smaller than t because of different types between two orbitals, imperfect lattice matches at the interface, and so on. When $E_{\rm F} = 0$, $e_{i,\uparrow}/|t|$ ($e_{i,\downarrow}/|t|$) is 5.1 (5.7) for FM1 and 5.175 (5.625) for FM2[6], by considering that the s orbital, which is spin-polarized by coupling to the localized d orbitals, contributes to the transport of the FMs. The spin polarization [15] at the interfacial layer of FM1 (FM2) at $E_{\rm F}$, P_1 (P_2), is then evaluated to be about 0.45 (0.25) [24][7]. For the carbon atom, $e_{i,\uparrow}/|t|$ ($e_{i,\downarrow}/|t|$) is set to be zero (zero) by focusing on its π orbital. By taking into account that the π orbital is coupled to d orbitals of the magnetic atoms, whose energies are lower than $e_{i,\uparrow}/|t|$ and $e_{i,\downarrow}/|t|$ of the π orbital, $\Delta e/|t|$ is considered to be positive and it is put as 0.2. Also, the number of unit cells in the circumference

[5] In the previous work [10], t was set to be -2.75 eV.

[6] To approximately describe the s electron within the tight-binding model, we consider that $E_{\rm F}$ is located near the bottom of an energy dispersion relation. The dispersion relation near the bottom is similar to that of the free electron, which is characteristic of the s electron. For example, see [23].

[7] Materials with $P_1 \sim 0.45$ correspond nearly to Co, Fe, and $Ni_{80}Fe_{20}$, while $P_2 \sim 0.25$ is Ni.

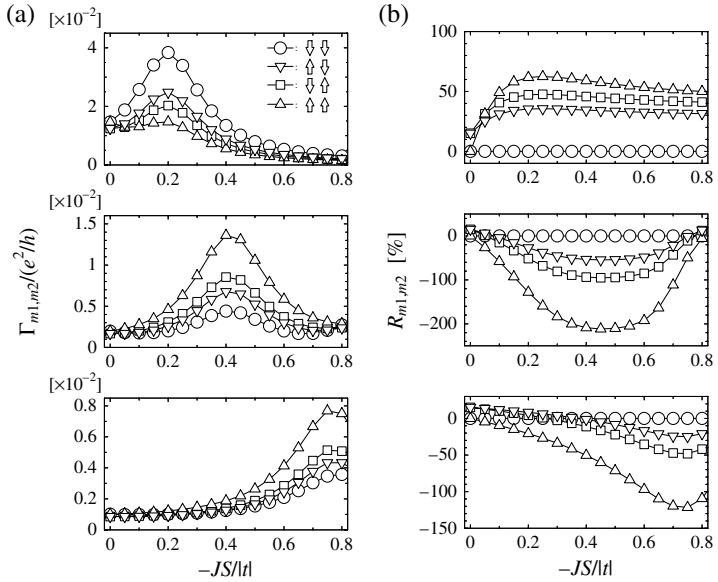

Figure 2. (a) The conductance $\Gamma_{m1,m2}$ versus $-JS/|t|$ for $\theta = 0$ and $\Delta e/|t| = 0.2$. The meanings of dots in all panels are ∘, $\Gamma_{\Downarrow,\Downarrow}$; ▽,: $\Gamma_{\Uparrow,\Downarrow}$; □, $\Gamma_{\Downarrow,\Uparrow}$; △, $\Gamma_{\Uparrow,\Uparrow}$. (b) The MR ratio $R_{m1,m2}$ versus $-JS/|t|$ for $\theta = 0$ and $\Delta e/|t| = 0.2$. In each figure, the upper, middle, and lower panels are cases of $N = 20$, 21, and 22, respectively. The meanings of dots in all panels are ∘,: $R_{\Downarrow,\Downarrow}$; ▽, $R_{\Uparrow,\Downarrow}$; □, $R_{\Downarrow,\Uparrow}$, and △, $R_{\Uparrow,\Uparrow}$.

direction of the nanotube is 10. The number of dimer lines [21] N is 20, 21, and 22, which correspond to nanotubes with the on-resonance, the off-resonance, and the off-resonance at E_F, respectively [10, 21]. It is well known that the armchair nanotube shows the on-resonant behaviour for $N = 3M - 1$, the off-resonant one for $N = 3M$, and the off-resonant one for $N = 3M + 1$, respectively, with M being an integer [10, 21]. For $N = 20$ and 21, the spin, **S**, is arrayed at each carbon atom in the 10th and 11th dimer lines of the nanotube, while it is arrayed at each carbon atom in its 11th and 12th dimer lines for $N = 22$. In each N, the number of spins **S** is 40, which is obtained from the relation of (the number of unit cells in the circumference direction of the nanotube) × (the number of dimer lines with spins **S**) × (the number of sublattices in the unit cell) = 10 × 2 × 2. Furthermore, spins **S** are considered to exist parallel to the yz-plane, and the angle between spins **S** and the z-axis is written as θ.

3.2. Calculated results and considerations

In the upper panel of figure 2(a), we show the $-JS/|t|$ dependence of the conductance, $\Gamma_{m1,m2}$, for $\theta = 0$ in the case of $N = 20$. At $JS/|t| = 0$, $\Gamma_{m1,m2}$ has a difference only between P and AP configurations. For $JS/|t| \neq 0$, differences among all conductances appear, and become largest in the vicinity of $JS/|t| = -0.2$. Also, $\Gamma_{m1,m2}$ has the relation $\Gamma_{\Downarrow,\Downarrow} > \Gamma_{\Uparrow,\Downarrow} > \Gamma_{\Downarrow,\Uparrow} > \Gamma_{\Uparrow,\Uparrow}$ for a wide range of $-0.8 < JS/|t| < 0$.

The middle and lower panels of figure 2(a) show $\Gamma_{m1,m2}$ for $\theta = 0$ in the casea of $N = 21$ and 22, respectively. In the case of $N = 21$, differences among all conductances become large in the vicinity of $JS/|t| = -0.4$, while they do in the vicinity of $JS/|t| = -0.75$ in the case of $N = 22$. It should be noted that $\Gamma_{m1,m2}$ of $N = 21$ and 22 has the relation $\Gamma_{\Uparrow,\Uparrow} > \Gamma_{\Downarrow,\Uparrow} > \Gamma_{\Uparrow,\Downarrow} > \Gamma_{\Downarrow,\Downarrow}$ for a wide range of $-0.8 < JS/|t| < 0$, and its order is opposite to that of $N = 20$.

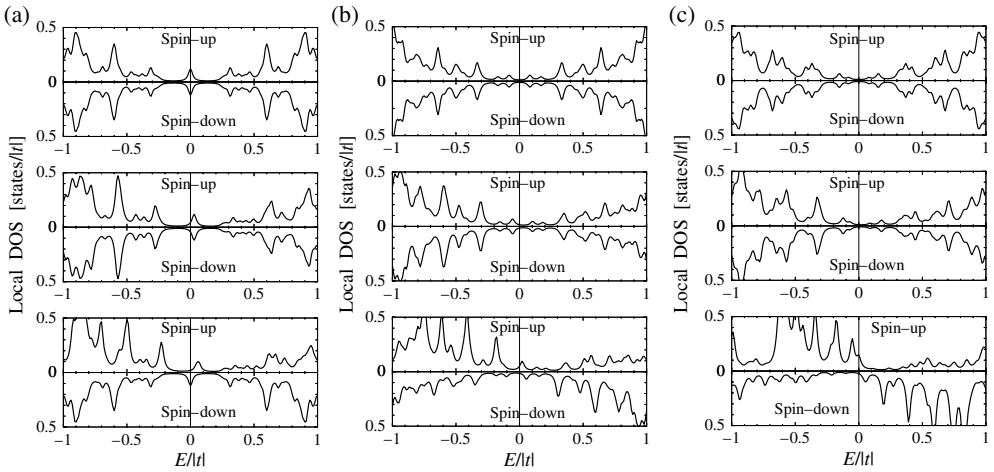

Figure 3. The local DOS in the centre of the nanotube, where magnetic atoms are encapsulated. (a) The case of $N = 20$. Upper panel: $\Delta e/|t| = 0$ and $JS/|t| = 0$. Middle panel: $\Delta e/|t| = 0.2$ and $JS/|t| = 0$. Lower panel: $\Delta e/|t| = 0.2$ and $JS/|t| = -0.2$. (b) The case of $N = 21$. Upper panel: $\Delta e/|t| = 0$ and $JS/|t| = 0$. Middle panel: $\Delta e/|t| = 0.2$ and $JS/|t| = 0$. Lower panel: $\Delta e/|t| = 0.2$ and $JS/|t| = -0.4$. (c) The case of $N = 22$. Upper panel: $\Delta e/|t| = 0$ and $JS/|t| = 0$. Middle panel: $\Delta e/|t| = 0.2$ and $JS/|t| = 0$. Lower panel: $\Delta e/|t| = 0.2$ and $JS/|t| = -0.8$. Here, $E_{\rm F} = 0$ is set.

The behaviour of conductances can be understood by considering electronic states in the centre of the nanotube, where magnetic atoms are encapsulated. We therefore investigate the local DOS, defined by

$$\text{Local DOS} = -\frac{1}{\pi}\,\text{Im}\sum_{i\in\text{mag}}\langle i|(E_{\rm F}+i0-H_{\rm NT})^{-1}|i\rangle, \tag{15}$$

where $|i\rangle$ represents the orbitals of carbon atoms interacting with magnetic atoms, and $\sum_{i\in\text{mag}}$ means that the summation is taken for those carbon atoms.

In the upper, middle, and lower panels of figure 3(a), we show the local DOS for $\Delta e/|t| = 0$ and $JS/|t| = 0$, $\Delta e/|t| = 0.2$ and $JS/|t| = 0$, and $\Delta e/|t| = 0.2$ and $JS/|t| = -0.2$, respectively, in the case of $N = 20$. For $\Delta e/|t| = 0$ and $JS/|t| = 0$, i.e., the case of no encapsulated atoms, small spin-up and spin-down peaks are found at $E_{\rm F}$ (=0), as shown in the upper panel of figure 3(a). The feature just represents the on-resonance at $E_{\rm F}$. The peaks originate from wavefunctions at the Gamma point [21], which are delocalized over the whole nanotube. For $\Delta e/|t| = 0.2$ and $JS/|t| = 0$, i.e., the case of encapsulated nonmagnetic atoms, the spin-up and spin-down peaks are shifted to higher energy with the same magnitude (see the middle panel of figure 3(a)). Then, two-valued conductances are obtained because of no difference of local DOSs between spin up and spin down. On the other hand, for $\Delta e/|t| = 0.2$ and $JS/|t| = -0.2$, i.e., the case of encapsulated magnetic atoms, the spin-down peak is close to $E_{\rm F}$ as shown in the lower panel of figure 3(a). Since the electron favours transmission when the DOS is large around $E_{\rm F}$, transmission of the spin-down electron increases compared to that of the spin-up electron. By taking into account the spin-dependent DOSs of FMs with $P_1 = 0.45$ and $P_2 = 0.25$, $\Gamma_{\Downarrow,\Downarrow}$ ($\Gamma_{\Uparrow,\Uparrow}$) becomes largest (smallest) in all conductances, while $\Gamma_{\Uparrow,\Downarrow}$ and $\Gamma_{\Downarrow,\Uparrow}$ are present between $\Gamma_{\Downarrow,\Downarrow}$ and $\Gamma_{\Uparrow,\Uparrow}$, and $\Gamma_{\Uparrow,\Downarrow} > \Gamma_{\Downarrow,\Uparrow}$ is also realized.

The upper, middle, and lower panels of figure 3(b) show the local DOS for $\Delta e/|t| = 0$ and $JS/|t| = 0$, $\Delta e/|t| = 0.2$ and $JS/|t| = 0$, and $\Delta e/|t| = 0.2$ and $JS/|t| = -0.4$,

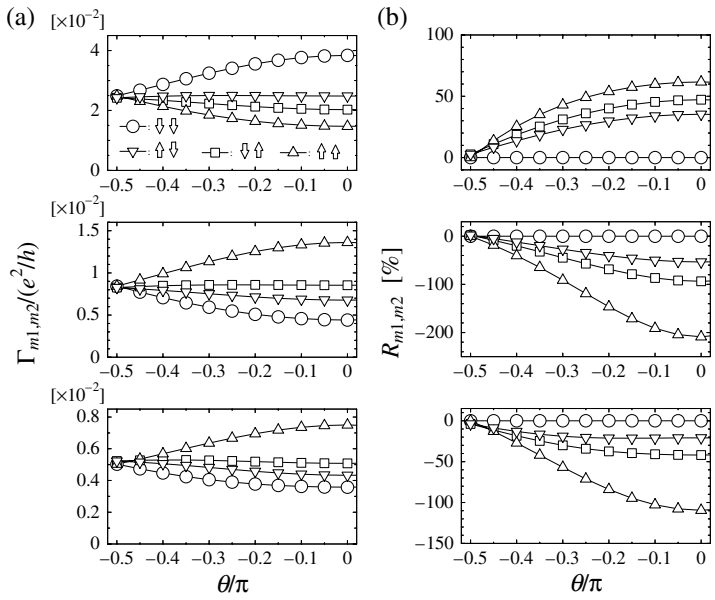

Figure 4. (a) The conductance $\Gamma_{m1,m2}$ versus θ. The meanings of symbols in all panels follow those of figure 2(a). (b) The MR ratio $R_{m1,m2}$ versus θ. In each figure, the upper, middle, and lower panels are cases of $JS/|t| = -0.2$ of $N = 20$, $JS/|t| = -0.4$ of $N = 21$, and $JS/|t| = -0.8$ of $N = 22$, respectively. The meanings of symbols in all panels follow those of figure 2(b).

respectively, in the case of $N = 21$. In the upper panel of figure 3(b), no peaks are found at E_F for $\Delta e/|t| = 0$ and $JS/|t| = 0$. This represents the off-resonance at E_F. By setting $\Delta e/|t| = 0.2$ and $JS/|t| = 0$, spin-up and spin-down peaks near E_F are shifted to higher energy with the same magnitude as shown in the middle panel of figure 3(b), and then two-valued conductances are obtained. For $\Delta e/|t| = 0.2$ and $JS/|t| = -0.4$, the spin-up peak appears in the vicinity of E_F (see the lower panel of figure 3(b)). Therefore, based on the DOSs of the FMs, $\Gamma_{\Uparrow,\Uparrow}$ ($\Gamma_{\Downarrow,\Downarrow}$) is largest (smallest) in all conductances, while $\Gamma_{\Uparrow,\Downarrow}$ and $\Gamma_{\Downarrow,\Uparrow}$ are present between $\Gamma_{\Uparrow,\Uparrow}$ and $\Gamma_{\Downarrow,\Downarrow}$, and $\Gamma_{\Downarrow,\Uparrow} > \Gamma_{\Uparrow,\Downarrow}$ is also realized. The case of $N = 22$ can be understood based on the local DOSs shown in figure 3(c), too.

We systematically understand the above peak shifts as follows: when the carbon atom interacts with the magnetic atoms, its spin-up energy levels are shifted to high energy, while its spin-down energy levels are not greatly altered, owing to $\Delta e/|t| > 0$ and $JS/|t| < 0$. For the on-resonant nanotube, in which spin-up and spin-down energy levels exist at E_F for $\Delta e/|t| = JS/|t| = 0$, the spin-down energy levels are closer to E_F than the spin-up ones when $\Delta e/|t| > 0$ and $JS/|t| < 0$. On the other hand, for the off-resonant nanotube, in which no spin-up and spin-down energy levels exist at E_F for $\Delta e/|t| = JS/|t| = 0$, the spin-up energy levels near the top of the valence band approach E_F by setting $\Delta e/|t| > 0$ and $JS/|t| < 0$.

The MR ratio $R_{m1,m2}$ is shown in figure 2(b). In all panels, at $JS/|t| = 0$, $R_{m1,m2}$ is finite only between P and AP configurations and $|R_{m1,m2}|$ is about 15%. For a wide range of $-0.8 < JS/|t| < 0$, $|R_{m1,m2}|$ between P and AP configurations can be more than 15%. It should be emphasized that $|R_{m1,m2}|$ between $\Uparrow$, $\Uparrow$ and $\Downarrow$, $\Downarrow$ is larger than the conventional one between P and AP configurations. This feature is consistent with results for the case of the largely spin-polarized spacer with $(T_{\uparrow,\uparrow} - T_{\downarrow,\downarrow})/T_{\uparrow,\uparrow} \sim 1$ in the previous work [14]. Also, it is characteristic that for a wide range of $-0.8 < JS/|t| < 0$, $R_{m1,m2}$-values of $N = 20$ and

21 and 22 exhibit the positive MR and the negative one, respectively, reflecting the opposite order of $\Gamma_{m1,m2}$ between them.

In the following, we consider the θ-dependence of $\Gamma_{m1,m2}$ and $R_{m1,m2}$, shown in figures 4(a) and (b), respectively. In each figure, the upper, middle, and lower panels are cases of $JS/|t| = -0.2$ of $N = 20$, $JS/|t| = -0.4$ of $N = 21$, and $JS/|t| = -0.8$ of $N = 22$, respectively. A condition of $\theta/\pi = -0.5$ (0) represents that spins **S** are oriented in the $-y$ (z) direction. In all panels, at $\theta/\pi = -0.5$, only the difference of $\Gamma_{m1,m2}$ between the P and AP configurations is present, and then $|R_{m1,m2}|$ between them takes small values of less than 5%, because of the spin-flip transmission. As θ approaches zero, differences of $\Gamma_{m1,m2}$ among all configurations become large, because the difference of diagonal elements of $\hat{T}$ with regards to spin between spin up and spin down increases. Further, $|R_{m1,m2}|$ between $\Uparrow$, $\Uparrow$ and $\Downarrow$, $\Downarrow$ increases, too.

4. Conclusion

For 'FM1/armchair carbon nanotube encapsulating magnetic atoms/FM2' junctions, we theoretically investigated the multiple-valued cell property which is in principle realized by sensing four states recorded with the magnetization configurations of two FMs. The obtained four-valued conductances are strongly influenced by electronic states of the nanotube, and directions of spins of magnetic atoms. The order of magnitude of four-valued conductances is opposite between the on-resonant nanotube and the off-resonant one. Furthermore, the MR ratio between (up, up) and (down, down) can be larger than the conventional one between P and AP configurations.

From the viewpoint of device applications, we expect that the present junctions will be a candidate for elements of the 2 bits/cell MRAM. At the same time, the junctions with magnetization reversals between $\Uparrow$, $\Uparrow$ and $\Downarrow$, $\Downarrow$ may be more efficient magnetic sensors than the conventional spin-valve type [5], in the case of the largely spin-polarized spacer.

Acknowledgments

This work has been supported by Special Coordination Funds for Promoting Science and Technology, Japan. One of the authors (KH) also acknowledges partial financial support from NEDO via the Synthetic Nano-Function Materials Project, AIST, Japan.

References

[1] Miyazaki T and Tezuka N 1995 *J. Magn. Magn. Mater.* **139** L231
Moodera J S, Kinder L R, Wong T M and Meservey R 1995 *Phys. Rev. Lett.* **74** 3273
[2] Tsunoda M, Nishikawa K, Ogata S and Takahashi M 2002 *Appl. Phys. Lett.* **80** 3135
[3] Tanaka M and Higo Y 2001 *Phys. Rev. Lett.* **87** 026602
[4] Jansen R and Moodera J S 1999 *Appl. Phys. Lett.* **75** 400
[5] For example, see Parkin S S, Roche K P, Samant M G, Rice P M, Beyers R B, Scheuerlein R E, O'Sullivan E J, Brown S L, Bucchigano J, Abraham D W, Lu Yu, Rooks M, Trouilloud P L, Wanner R A and Gallagher W J 1999 *J. Appl. Phys.* **85** 5828
[6] Tsukagoshi K, Alphenaar B W and Ago H 1999 *Nature* **401** 572
[7] Zhao B, Mönch I, Mühl T, Vinzelberg H and Schneider C M 2002 *Appl. Phys. Lett.* **80** 3144
[8] Zhao B, Mönch I, Mühl T, Vinzelberg H and Schneider C M 2002 *J. Appl. Phys.* **91** 7026
[9] Kim J-R, So H M, Kim J-J and Kim J 2002 *Phys. Rev.* B **66** 233401
[10] Mehrez H, Taylor J, Guo H, Wang J and Roland C 2000 *Phys. Rev. Lett.* **84** 2682
[11] Kokado S and Harigaya K 2004 *Phys. Rev.* B **69** 132402
Kokado S and Harigaya K 2003 *Synth. Met.* **135** 745

[12] For example, see Takahashi N, Ishikuro H and Hiramoto T 2000 *Appl. Phys. Lett.* **76** 209
[13] Giridhar R V 1996 *Japan. J. Appl. Phys.* **35** 6347
[14] Kokado S and Harigaya K 2003 *J. Phys.: Condens. Matter* **15** 8797
[15] De Teresa J M, Barthelemy A, Fert A, Contour J P, Montaigne F and Seneor P 1999 *Science* **286** 507
[16] For carbon nanotubes encapsulating magnetic atoms at the edge, Zhang X X, Wen G H, Huang S, Dai L, Gao R and Wang Z L 2001 *J. Magn. Magn. Mater.* **231** L9
[17] For carbon nanotubes encapsulating magnetic atoms in the inner region, Zhao X, Inoue S, Jinno M, Suzuki T and Ando Y 2003 *Chem. Phys. Lett.* **373** 266
[18] Todorov T N, Briggs G A D and Sutton A P 1993 *J. Phys.: Condens. Matter* **5** 2389
[19] Kokado S, Ichimura M, Onogi T, Sakuma A, Arai R, Hayakawa J, Ito K and Suzuki Y 2001 *Appl. Phys. Lett.* **79** 3986
[20] Ichiyanagi Y and Kimishima Y 2002 *J. Therm. Anal. Cal.* **69** 919
As a relevant report, see Ichiyanagi Y, Uozumi T and Kimishima Y 2001 *Trans. Mater. Res. Soc. Japan* **26** 1097
[21] Wakabayashi K, Fujita M, Ajiki H and Sigrist M 1999 *Phys. Rev.* B **59** 8271
[22] Schrieffer J R and Wolff P A 1966 *Phys. Rev.* **149** 491
[23] Itoh H, Shibata A, Kumazaki T, Inoue J and Maekawa S 1999 *J. Phys. Soc. Japan* **68** 1632
[24] Moodera J S and Mathon G 1999 *J. Magn. Magn. Mater.* **200** 248